# ORIGINAL RESEARCH

Deletion of C-C Motif Chemokine Ligand 5 Worsens Invariant Natural Killer T-Cell–Mediated Hepatitis via Compensatory Up-regulation of CXCR2–Related Chemokine Activity

Lili Chen,[1,2,a] Jinyang Gu,[3,a] Yihan Qian,[4,a] Meng Li,[2,a] Yongbing Qian,[2] Min Xu,[2] Jichang Li,[2] Yankai Wen,[2] Lei Xia,[2] Jiaxin Li,[2] Qiang Xia,[2] Xiaoni Kong,[2] and Hailong Wu[1]

[1]Shanghai Key Laboratory for Molecular Imaging, Collaborative Research Center, Shanghai University of Medicine and Health Sciences, Shanghai, China; [2]Department of Liver Surgery, Renji Hospital, School of Medicine, Shanghai Jiao Tong University, Shanghai, China; [3]Department of Transplantation, Xinhua Hospital, School of Medicine, Shanghai Jiao Tong University, Shanghai, China; and [4]School of Pharmacy, Fudan University, Shanghai, China
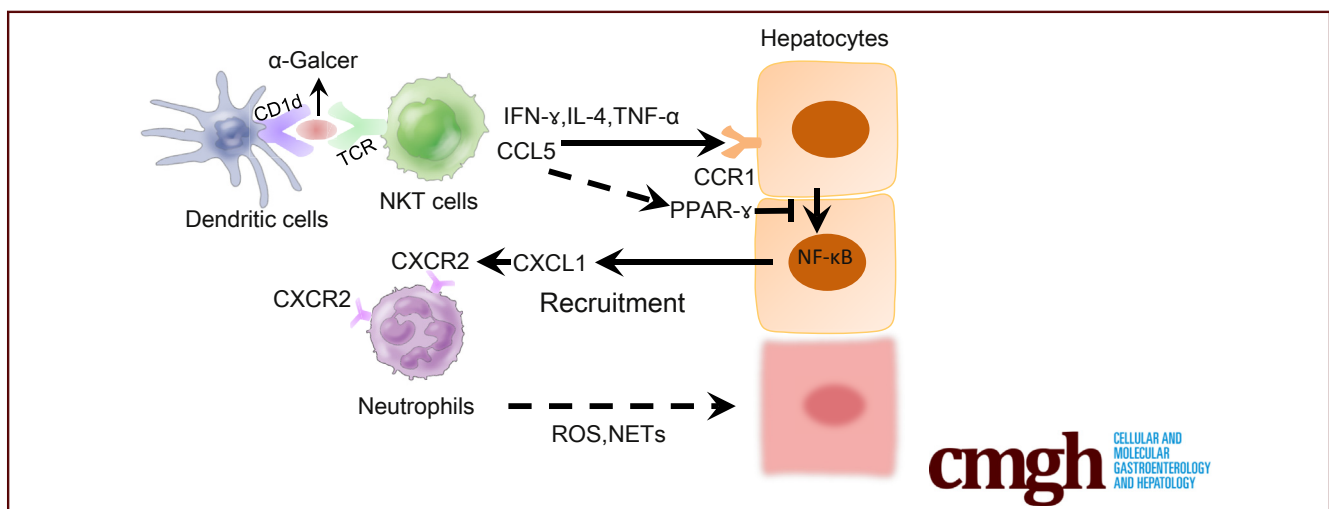
SUMMARY

This study reports that deficiency of *Ccl5*, one of CC chemokine family proteins, augments invariant NKT mediated hepatitis. Genetic loss of *Ccl5* does not affect iNKT activation directly but significantly elevates CXCL1 expression in hepatocytes, which sequentially leads to increased hepatic neutrophil infiltration in a CXCL1-CXCR2 dependent manner and results in enhanced hepatitis.

BACKGROUND & AIMS: Chemokine-mediated immune cell recruitment plays pivotal roles in liver inflammation. C-C motif chemokine ligand 5 (CCL5) has been shown to be responsible for the recruitment of monocytes/macrophages and has been implicated in various liver diseases, including nonalcoholic fatty liver disease, fibrosis, and hepatocellular carcinoma. Previous studies have also shown that inhibition of CCL5 appears to be a promising therapeutic approach for several chronic liver diseases. However, whether blocking CCL5 could benefit immune cell–mediated hepatitis remains largely elusive.

METHODS: By adopting a specific agonist, alpha-galactosylceramide (α-Galcer), of invariant natural killer T cells (iNKTs), we investigated the function and mechanism of CCL5 in the iNKT induced murine hepatitis model.

RESULTS: We found significantly increased CCL5 expression in α-Galcer–induced hepatitis murine model. Such an increase in CCL5 is mainly enriched in non-parenchymal cells such as macrophages and iNKTs but not in hepatocytes. Surprisingly, CCL5 blockage by genetic deletion of *Ccl5* does not affect the α-Galcer–induced iNKT activation but greatly worsens α-Galcer–induced liver injury accompanied by an increased hepatic neutrophil infiltration. Mechanistically, we demonstrated that greater neutrophil accumulation in the liver is responsible for the enhanced liver injury in *Ccl5*$^{-/-}$ mice. Such an increased hepatic neutrophil infiltration is mainly caused by an enhanced CXCL1-CXCR2 signal in *Ccl5*$^{-/-}$ mice. Therapeutically, either antibody-mediated neutrophil depletion or a CXCR2 antagonist, SB225002, mediated CXCR2 signaling blockage significantly ameliorated α-Galcer–induced liver injury in *Ccl5*$^{-/-}$ mice.

CONCLUSIONS: Our present study demonstrates that (1) α-Galcer–induced murine hepatitis could greatly induce CCL5 production in macrophages and iNKT cells; (2) loss of CCL5 could enhance CXCL1 expression in hepatocytes and activate CXCL1-CXCR2 axis in neutrophils to augment their hepatic

infiltration; and (3) neutrophil depletion or blockage of CXCL1-CXCR2 axis greatly improves α-Galcer–induced liver injury in *Ccl5*^{-/-} mice. This study suggests that clinical utilization of CCL5 blockage may compensatorily induce the activation of other chemokine pathways to enhance neutrophil recruitment and liver injury in hepatitis. *(Cell Mol Gastroenterol Hepatol 2019;7:623–639; https://doi.org/10.1016/j.jcmgh.2018.12.009)*

Liver diseases are generally accompanied with inflammatory responses. Hepatic inflammation is a key factor for the progression of both acute and chronic liver diseases, including viral hepatitis, nonalcoholic fatty liver disease (NAFLD), liver fibrosis, and hepatocellular carcinoma (HCC).[1] Chemokines and their receptors play important roles in development of hepatic inflammation by regulating hepatic infiltration of circulating inflammatory cells, which can lead to either inflammation enhancement or resolution.[2] Chemokines can also exert direct biologic alteration on hepatic stellate cells (HSCs) to induce their migration and activation of intracellular signaling pathways.[3]

C-C motif chemokine ligand 5 (*Ccl5*), also known as RANTES, belongs to CC chemokine family and has been reported to be induced in several liver diseases in humans including acute liver failure, chronic liver disease, NAFLD, viral hepatitis, fibrosis, and HCC.[4] CCL5 recruits leukocyte migration via binding its receptors CCR1, CCR3, or CCR5. In addition, the role of CCL5 in liver diseases has also been elucidated in various animal models. For example, elevated CCL5 production was found in hepatic ischemia/reperfusion injury,[5] ethanol-induced liver injury,[6] and concanavalin A–induced hepatitis model.[7,8] In CCR5 deficiency mice, T-cell–mediated hepatitis was exacerbated, where CCL5, as a CCR5 ligand, promotes the recruitment of liver mononuclear cells, especially interferon (IFN)-γ producing natural killer (NK) cells to the liver of *Ccr5*^{-/-} mice via CCR1.[7,8] Genetic loss of *Ccl5* or CCL5 blockage by met-CCL5, a CCL5 antagonist, alleviated experimental hepatic fibrosis in mice induced by either carbon tetrachloride administration or methionine and choline–deficient diet feeding.[9,10] Hepatic CCL5 production was increased and accompanied with significant hepatic steatosis in the high-fat diet–induced NAFLD model.[11] In addition, it has also been shown that CCL5 promotes HCC progression in mice.[12,13]

Natural killer T cells (NKTs) are extremely abundant and predominantly reside in the liver sinusoids.[14,15] Accumulating evidence suggests that NKTs are involved in the pathologic processes of many liver diseases, such as virus infection hepatitis, autoimmune liver diseases, alcoholic liver disease, NAFLD, liver fibrosis, and HCC.[16] This involvement is likely a direct result of the wide variety of cytokines, including IFN-γ, interleukin (IL) 4, IL 17, and tumor necrosis factor (TNF) α, which are produced by NKTs, as well as an indirect effect to induce production of chemokines that direct hepatic recruitment of many types of immune cells.[17]

NKTs are a population of nonconventional T lymphocytes that share phenotypic and functional characteristics with both conventional T cells and NK cells. NKTs specifically recognize lipid antigens that are mainly presented by CD1d, a non-canonical major histocompatibility complex class I-like molecular. According to their T-cell receptors diversity, NKTs can be categorized into 2 subsets: type I (invariant NKT [iNKT]) and type II NKT cells.[18] Alpha-galactosylceramide (α-Galcer) is a specific ligand to activate iNKTs and induce iNKTs to produce a variety of cytokines. Although α-Galcer has been investigated in many clinical studies for the treatment of viral hepatitis and liver cancer,[19] its application has been limited because of the difficulties to decipher which are the key factors contributing to the α-Galcer–induced progression of hepatitis. In a recent study, Wang et al[20] sophisticatedly proposed a model in which IL4 and IFN-γ act as the "gas" and "brake" to enhance or ameliorate, respectively, iNKT hepatitis by promoting neutrophil survival or apoptosis, suggesting a central role of neutrophil in iNKT mediated hepatitis.

Although CCL5 has been studied in various acute and chronic liver diseases, little is known about its role in iNKT mediated hepatitis. In the present study, we found that CCL5 expression is significantly increased in the α-Galcer–induced hepatitis mouse model. Genetic deletion of *Ccl5* promotes α-Galcer–induced liver injury, which is paralleled with increased hepatic neutrophil infiltration. Mechanistically, CCL5 deficiency up-regulates CXCL1 levels in hepatocytes and in turn enhances hepatic neutrophil infiltration in a CXCR2 dependent manner.

Results
C-C Motif Ligand 5 Is Up-regulated in the Alpha-galactosylceramide–Induced Mouse Hepatitis Model

Immune cell–mediated hepatic injury is involved in a variety of liver diseases triggered by viral hepatitis or autoimmune hepatitis (AIH). In those diseases, chemokines could be a crucial group of pathogenic factors via directing hepatic infiltration of many types of immune cells.[21,22] To evaluate the association of CCL5 with hepatitis, we first

[a]Authors share co-first authorship.

Most current article

measured hepatic CCL5 expression in patients with either viral hepatitis or AIH. Immunohistochemical staining showed that the CCL5 levels were highly elevated in the liver of patients with chronic type B (hepatitis B virus [HBV]), type C hepatitis (hepatitis C virus [HCV]), or AIH (Figure 1A), compared with the plain staining in healthy controls, where CCL5 was expressed in both hepatocytes and immune infiltrating cells. In the α-Galcer–induced murine hepatitis model, mice showed rapidly elevated serum CCL5 levels, with a peak at 16 hours after injection (Figure 1B). Serum levels of IFN-γ and IL4 were also detected as their involvement in α-Galcer induced hepatitis.[20] As shown in Figure 1B, IFN-γ increased after α-Galcer treatment with a peak at 16 hours, whereas IL4 peaked at 3 hours after injection. Although elevated CCL5 expression was found in both hepatocytes and non-parenchymal cells (NPCs) by quantitative real-time polymerase chain reaction (PCR) analysis after α-Galcer stimulation, *Ccl5* mRNA levels were much higher in NPCs than those in hepatocytes (Figure 1C), suggesting that CCL5 derived from NPCs may mainly contribute to α-Galcer–induced hepatic CCL5 elevation. In NPCs, *Ccl5* expression significantly increased in macrophages and NKTs but showed no changes in HSCs after α-Galcer treatment (Figure 1C and D). These findings indicated that NKTs and macrophages are the main cell sources of CCL5 elevation in α-Galcer–induced hepatitis.

Deletion of C-C Motif Chemokine Ligand 5 Exacerbates Alpha-galactosylceramide–Induced Liver Injury and Hepatitis

To examine the function of CCL5 in iNKT induced hepatitis, both wild-type (WT) and *Ccl5*^{-/-} mice were treated with α-Galcer for 24 and 72 hours. WT mice showed mild liver injury with the presence of macroscopic white spots on the liver. To our surprise, α-Galcer induced much more severe liver injury in *Ccl5*^{-/-} mice as evidenced by more macroscopic white spots on the liver 24 and 72 hours after injection compared with WT mice (Figure 1E). Consistently, α-Galcer treatment slightly elevated serum alanine aminotransferase (ALT) and aspartate aminotransferase (AST) levels in WT mice but induced greater serum ALT and AST release in *Ccl5*^{-/-} mice (Figure 1F and G). In line with the ALT/AST level differences between WT and *Ccl5*^{-/-} mice, H&E staining indicated that α-Galcer induced a higher grade of inflammatory foci and necrotic areas in the liver of *Ccl5*^{-/-} mice than in WT mice (Figure 1H and I). These findings indicated *Ccl5* depletion worsens α-Galcer–induced liver injury and hepatitis.

C-C Motif Chemokine Ligand 5 Deficiency Does Not Directly Affect Alpha-galactosylceramide–Induced Invariant Natural Killer T-Cell Activation and Inflammatory Cytokine Production in Splenocytes

Considering that α-Galcer is an agonist specifically inducing iNKT activation and the production of cytokines such as IFN-γ, IL4, and TNF-α, we evaluated iNKT population in WT and *Ccl5*^{-/-} mice by analyzing CD3 and NK1.1

levels. Flow cytometry assays revealed that the percentages of CD3^{+}NK1.1^{+} cells in either WT or *Ccl5*^{-/-} mice were no different and decreased rapidly after α-Galcer treatment (Figure 2A), which is consistent with previous reports.[23,24] Moreover, co-staining of early activation marker CD69 also showed no difference in CD3^{+}NK1.1^{+} NKTs in both WT and *Ccl5*^{-/-} mice (Figure 2B). To further confirm these in vivo results, we used CD3 and tetrameric CD1d molecules loaded with α-Galcer (CD1d-α-Galcer tetramers, CD1d-tet) to identify the iNKT cells and co-staining with CD69 to evaluate their activation status. Similar to our in vivo findings, 3 hours after α-Galcer injection, iNKT populations and activation status in hepatic mononuclear cells (MNCs) (Figure 2C) or splenocytes (Figure 2D) were no different between 2 strains. In line with those findings, the production of IFN-γ and IL4 was comparable in both WT and *Ccl5*^{-/-} mice 3 hours after α-Galcer injection (Figure 2E and F), whereas IFN-γ was slightly higher in WT serum 16 and 24 hours after α-Galcer injection.

Because α-Galcer is a well-established ligand promoting iNKT activation, an in vitro stimulation system could be used to investigate the direct role of CCL5 on iNKT activation. In vitro stimulation of WT and *Ccl5*^{-/-} splenocytes by α-Galcer led to comparable production of IL4 and IFN-γ as evidenced by both quantitative real-time PCR (Figure 2G) and enzyme-linked immunosorbent assays (ELISAs) (Figure 2H). Collectively, these data demonstrate that CCL5 deficiency does not directly affect the population and activation of iNKTs.

Excessive Hepatic Neutrophil Infiltration Is Responsible for the Enhanced Liver Injury in C-C Motif Chemokine Ligand 5[-/-] Mice After Alpha-galactosylceramide Administration

The above findings indicated that WT and *Ccl5*^{-/-} mice had a similar population and activation status of iNKT cells after α-Galcer injection, suggesting that iNKTs are not attributed to the enhanced liver injury in *Ccl5*^{-/-} mice after α-Galcer. A recent study has shown that increased hepatic neutrophil infiltration greatly contributes to iNKT mediated hepatitis.[20] We then examined hepatic neutrophil infiltration of WT and *Ccl5*^{-/-} mice after α-Galcer injection. In line with previous findings, α-Galcer treatment caused an increase in hepatic neutrophils in both WT and *Ccl5*^{-/-} mice. As shown in Figure 3A and B, flow cytometry assays showed that the percentage of CD11b^{+}Gr-1^{+} neutrophils was elevated 3-fold in WT mice and 5-fold in *Ccl5*^{-/-} mice as early as 3 hours after α-Galcer injection. Moreover, the total number of hepatic neutrophils in *Ccl5*^{-/-} mice was also higher than that in WT mice after α-Galcer administration. In addition, immunohistochemical staining of myeloperoxidase (MPO) also showed greater hepatic MPO[+] neutrophils in *Ccl5*^{-/-} mice than in WT mice after α-Galcer injection (Figure 3 C and D). By examining the percentage of neutrophils in bone marrow and spleen, we demonstrated that CCL5 deficiency did not affect the neutrophil population in those organs 3 hours after α-Galcer injection (Figure 3E and F), suggesting that the increased hepatic neutrophils in *Ccl5*^{-/-} mice are mainly attributed to enhanced neutrophil recruitment.
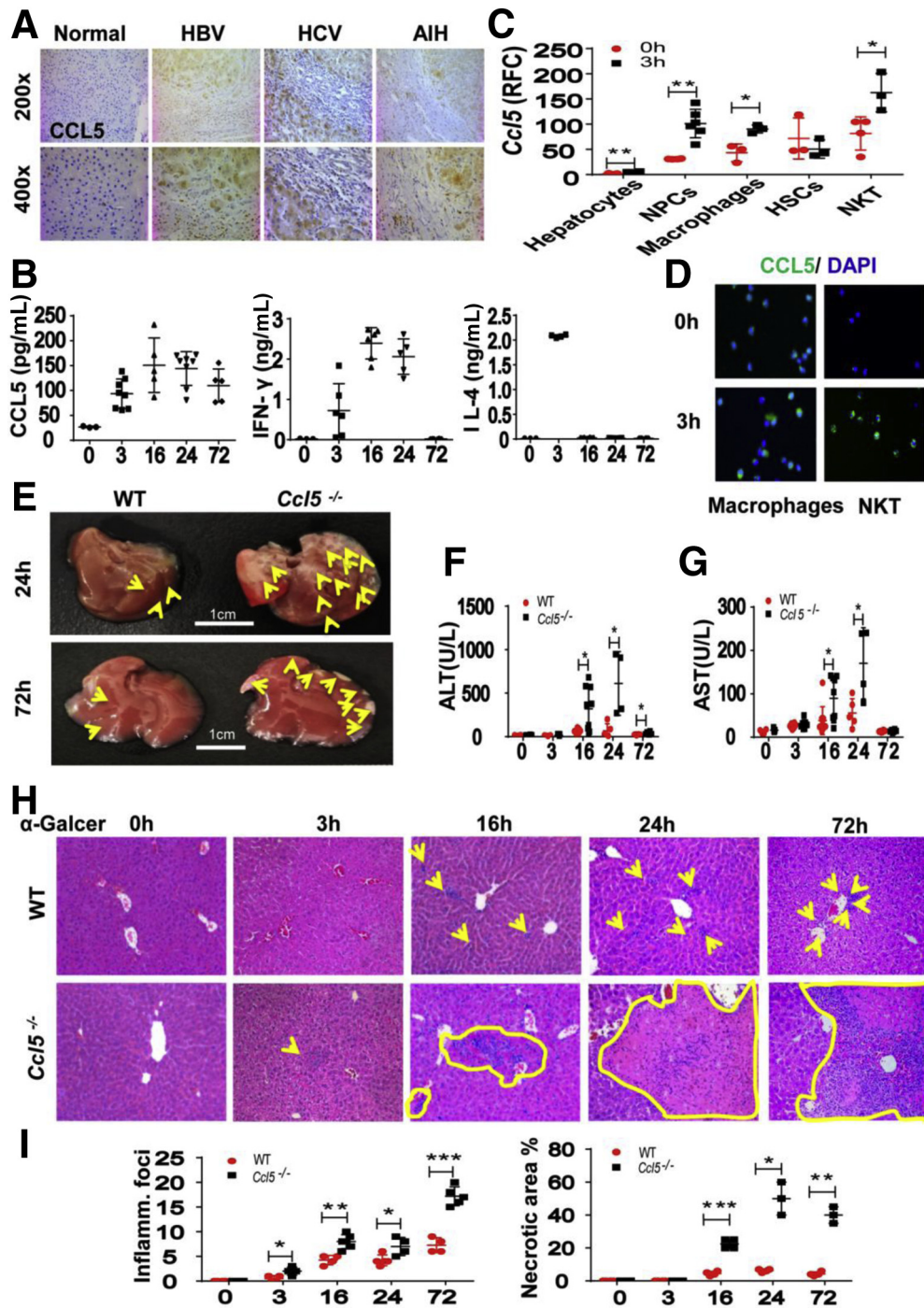
Figure 1. Up-regulation of CCL5 in human hepatitis and mouse model of experimental hepatitis and loss of CCL5 contribute to enhanced α-Galcer–induced hepatic injury. (*A*) Representative immunohistochemical staining hepatic CCL5 expression in normal human liver, chronic type B hepatitis, chronic type C hepatitis, and AIH. Original magnification, ×200 and ×400. (*B*) WT mice were treated with α-Galcer, and serum CCL5, IFN-γ, and IL4 levels were measured. (*C*) Relative expression of *Ccl5* was determined in primary hepatocytes and NPCs, macrophages, HSCs, and NKT cells isolated from α-Galcer–induced WT mice. (*D*) Immunofluorescence staining of CCL5 in macrophages and NKT cells. Original magnification, ×200. (*E*) Representative images of livers of WT and *Ccl5*−/− mice treated with 2 µg/mouse α-Galcer for 24 and 72 hours showing macroscopic signs of mild and severe liver injury, respectively. Sera were collected for measurement of ALT (*F*) and AST (*G*). (*H*) Representative H&E staining of liver tissue from α-Galcer–treated mice (original magnification, ×200). *Arrows* indicate inflammatory foci. *Yellow dotted line* indicates area of necrosis. (*I*) Graphs represent mean score of inflammatory foci and necrotic area for each group of mice. *$P < .05$, **$P < .01$, ***$P < .001$.
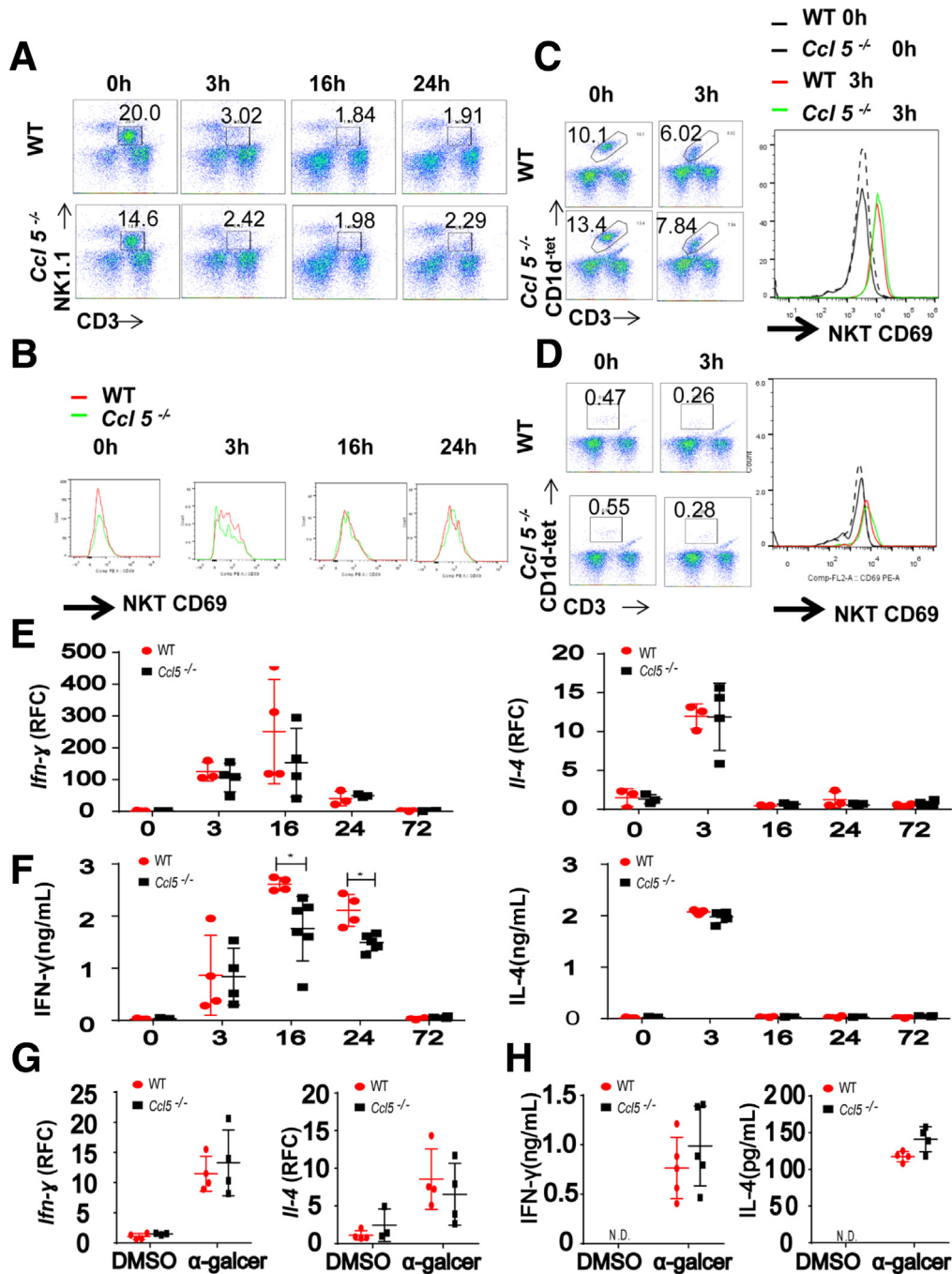
Figure 2. ***Ccl5* deficiency does not directly affect NKT cells activation and production of inflammatory cytokines.** WT and *Ccl5*^{-/-} mice were treated with α-Galcer, kinetics frequency of liver NKT cell accumulation (*A*) and activation status (*B*) in hepatic MNCs as defined by co-expression of CD3^{int}NK1.1^{+} (gated in CD45^{+} liver lymphocytes) and CD69 (gated in CD3^{int}NK1.1^{+}), respectively. Flow cytometry profiles are representative of mice (n = 5–6) per group. (*C*) WT and *Ccl5*^{-/-} mice were treated with α-Galcer for 3 hours, kinetics frequency of liver NKT cell accumulation and activation status in hepatic MNCs as defined by co-expression of CD3^{int}CD1d[-tet+] (gated in CD45^{+} liver lymphocytes) and CD69 (gated in CD3^{int}CD1d[-tet+]), respectively. Flow cytometry profiles are representative of mice (n = 5–6) per group. (*D*) Kinetics frequency of spleen NKT cell accumulation and activation status in MNCs as defined by co-expression of CD3^{int}CD1d[-tet+] (gated in CD45^{+} liver lympho-cytes) and CD69 (gated in CD3^{int}CD1d[-tet+]), respectively. Flow cytometry (FACS) profiles are representative of mice (n = 5–6) per group. (*E*) Mice were treated with α-Galcer for 3, 16, 24, and 72 hours, liver tissues were collected, and total RNA was isolated and subjected to real-time PCR analysis for *Ifn-γ* and *Il4*. (*F*) Serum was collected and measured for IFN-γ and IL4 by ELISA. (*G*) Spleen MNCs were cultured with α-Galcer for 6 hours. Relative expression of *Ifn-γ* and *Il4* was determined by quantitative real-time PCR. Data are representative of 3 independent experiments. (*H*) Spleen MNCs were cultured with α-Galcer for 24 hours. Expression of IFN-γ and IL4 in supernatant was determined by ELISA. Data are representative of 3 independent experiments. DMSO, dimethyl sulfoxide.
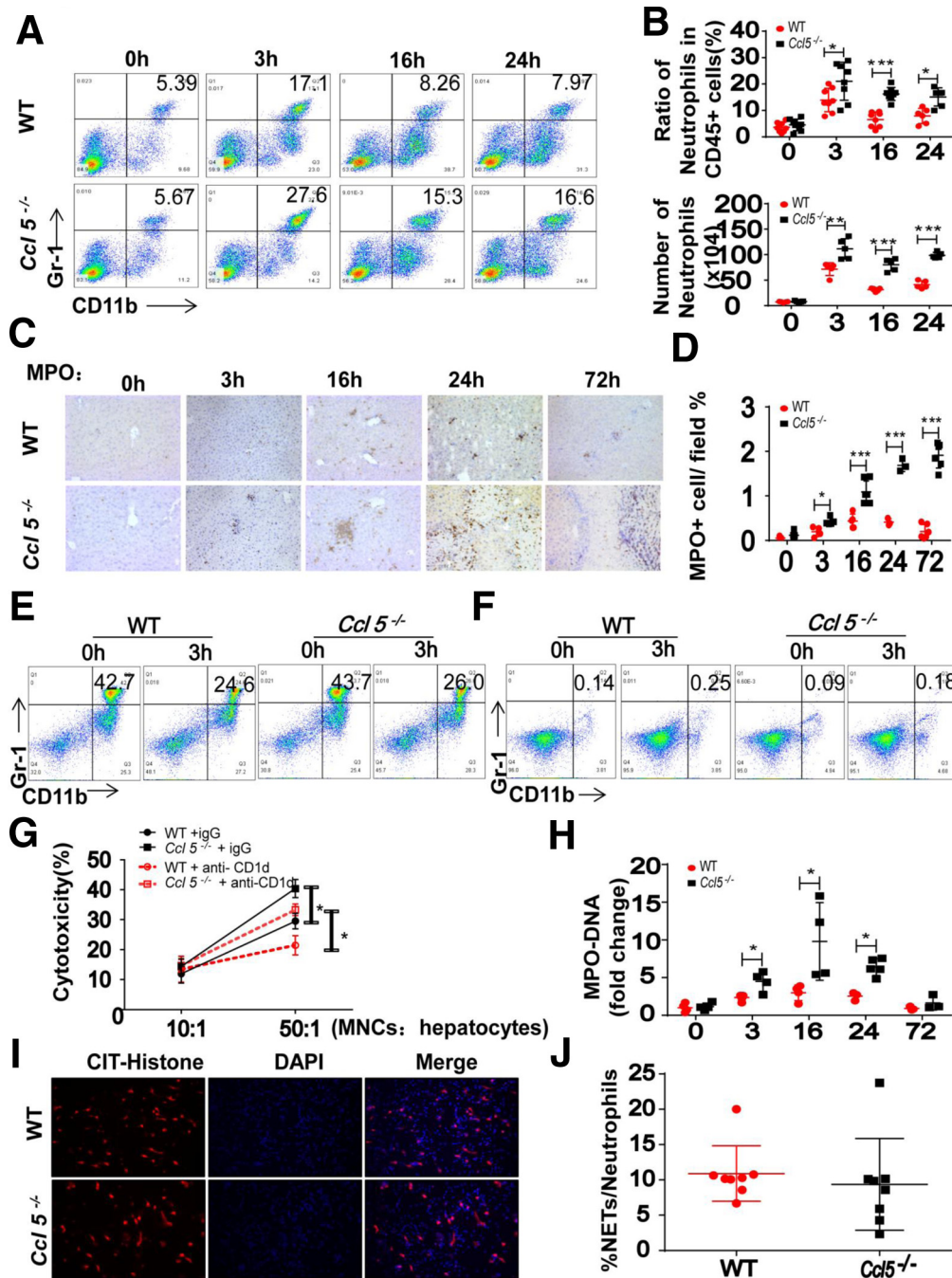
Figure 3. Neutrophils were accumulated higher in Ccl5^{-/-} mice. (A) Representative flow cytometry profiles showing percentages of neutrophils (CD11b^{high} Gr1^{high}) gated in CD45^{+} hepatic MNCs from WT and CCL5^{-/-} mice on α-Galcer treatment. (B) Graph with percentages (upper panel) and absolute numbers (lower panel) of neutrophils/10[6] hepatic MNCs in WT and CCL5^{-/-} mice during different phases of α-GalCer treatment (n = 5–6 mice per group). (C) Representative anti-MPO antibody–stained liver sections from α-GalCer–treated mice (original magnification, ×200). (D) Areas of MPO+ staining from (C) were quantified. Representative flow cytometry profiles showing percentages of neutrophils (CD11b highGr1high) gated in CD45+ hepatic MNCs from (E) bone marrow and (F) spleen in WT and Ccl5[-/] mice on α-Galcer treatment. (G) Hepatic MNCs were isolated from α-Galcer–treated (16 hours) WT and Ccl5^{-/-} mice and incubated with primary WT mouse hepatocytes for 2 hours. Meanwhile, 10 μg/mL anti-CD1d monoclonal antibody and rat immunoglobulin G1 isotype control were added in the medium. Cytotoxicity was measured. Experiments were performed independently 3 times. (H) NETs form after 3, 16, 24, and 72 hours of α-Galcer treatment, as assessed by serum level of MPO-DNA complex. Results are expressed as relative folds increase of MPO-DNA complex compared with control mice. (I) Bone marrow neutrophils were isolated from WT mice and stimulated with 100 nmol/L phorbol myristate acetate for 4 hours. Representative immunofluorescent staining images of cit-Histone and DAPI are shown. Original magnification, ×200. (J) Quantification of NETs formation per field was conducted. *P < .05, **P < .01, ***P < .001.

Next we examined the cytotoxicity of hepatic MNCs against hepatocytes. As illustrated in Figure 3*G*, 16 hours after α-Galcer injection, hepatic MNCs isolated from *Ccl5*^{-/-} mice showed higher level of cytotoxic activity against primary hepatocytes than from WT mice. After NKT depletion with anti-CD1d, higher cytotoxic activity was still observed from hepatic MNCs isolated from *Ccl5*^{-/-} mice but not from WT mice.

After infiltrating into inflammation sites, neutrophil-mediated hepatocyte injury could be achieved through releasing proinflammatory mediators, reactive oxygen species (ROS), as well as proteolytic enzymes.[25] We first checked whether there was higher ROS accumulation in neutrophils in *Ccl5*^{-/-} mice. No significant difference was found in ROS generation between WT and *Ccl5*^{-/-} neutrophils as detected by ROS indicators such as carboxy-2′,7′-dichlorodihydrofluorescein diacetate, MitoSOX, and malondialdehyde (data not shown).

Recent findings have reported that neutrophil extracellular traps (NETs) are a type of harmful contributor in neutrophil mediated liver injury.[26,27] However, the role of NET formation in α-Galcer–induced hepatitis remains unknown. To investigate whether NETs also contribute to the enhanced liver injury in α-Galcer–treated *Ccl5*^{-/-} mice, we measured serum NET levels in both WT and *Ccl5*^{-/-} mice by detecting the levels of MPO-DNA complexes (a hallmark of NET formation). We found that the levels of MPO-DNA significantly increased in both strains 3 hours after α-Galcer treatment, suggesting the activation of neutrophils (Figure 3*H*). In line with the finding that *Ccl5*^{-/-} mice have greater hepatic infiltration of neutrophils, the serum MPO-DNA levels were significantly higher in *Ccl5*^{-/-} mice than in WT mice (Figure 3*H*). Next we asked whether the deletion of *Ccl5* in neutrophil directly affects the NET formation. Immunofluorescence analysis of phorbol 1,2-myristate 1,3-acetate–induced NETs revealed that the degree of NETs was comparable in WT and *Ccl5*^{-/-} neutrophils (Figure 3*I* and *J*), suggesting that the increase in serum NET levels in *Ccl5*^{-/-} mice is simply due to increased hepatic neutrophil infiltration but not caused by increased NET formation in *Ccl5*^{-/-} neutrophils.

To answer whether the increased hepatic neutrophils contribute to enhanced liver injury in *Ccl5*^{-/-} mice after α-Galcer treatment, we performed a neutrophil depletion assay by using an anti-Ly6G antibody. As shown in Figure 4*A*, compared with isotype control, CD11b^{+}Gr-1^{+} neutrophils were completely depleted by the addition of anti-Ly6G antibody. Moreover, neutrophil depletion greatly protected the *Ccl5*^{-/-} mice from α-Galcer–induced hepatitis as evidenced by decreased presence of macroscopic white spots, inflammation foci, necrosis areas, and ALT/AST levels (Figure 4*B*–*F*). These results suggest that increased hepatic infiltration of neutrophils was responsible for the enhanced liver injury in *Ccl5*^{-/-} mice after α-Galcer administration.

C-C Motif Chemokine Ligand 5 Deficiency Synergistically Up-regulates Neutrophil Infiltration in Peripheral Blood

It is possible that *Ccl5* deficiency may also affect lymphocyte development,[28,29] resulting in the hypersensitivity of *Ccl5*^{-/-} mice to α-Galcer–induced hepatitis. To exclude this possibility, we determined the numbers of neutrophils (CD11b^{+}Gr-1^{+}), macrophages (CD45^{+}F4/80^{+}), NK cells (CD45^{+}NK1.1^{+}), dendritic cells (CD45^{+}CD11c^{+}), and B cells (CD45^{+}CD19^{+}) in bone marrow from adult WT and *Ccl5*^{-/-} mice. There were no significant differences in the percentages of those lymphocytes between both strains, which indicate that CCL5 deficiency does not affect the development of lymphocytes (data not shown).

It has been reported that CCL5 has no chemotactic effects directly on neutrophils.[30] To further explore the mechanism by which CCL5 deficiency induces hepatic neutrophil accumulation, we examined the levels of circulating neutrophils and chemokines responsible for hepatic neutrophil infiltration. As shown in Figure 5*A* and *B*, the percentage and total number of CD11b^{+}Gr-1^{+} neutrophils were rapidly increased in peripheral blood after α-Galcer administration in both strains but were much higher in *Ccl5*^{-/-} mice than in WT mice. Furthermore, after 3 hours of α-Galcer treatment, hepatic expression of neutrophil chemokine *Cxcl1* was up-regulated by 150-fold in *Ccl5*^{-/-} mice and 100-fold in WT mice. Other chemokines, chemokine receptors, and adhesion molecules were also up-regulated, but without significant differences in both strains (Figure 5*C* and *E*). Consistently, the serum levels of CXCL1 were also greatly up-regulated in WT and *Ccl5*^{-/-} mice 3 hours after α-Galcer injection and decreased in 6, 12, and 24 hours (Figure 5*D*). Moreover, the serum CXCL1 levels in *Ccl5*^{-/-} mice were significantly higher than in WT mice. Collectively, these findings suggest that elevated serum CXCL1 levels may contribute to increased liver neutrophil recruitment in *Ccl5*^{-/-} mice after α-Galcer treatment.

C-C Motif Chemokine Ligand 5 Regulates CXCL1 Production in Both Hepatocytes and Non-parenchymal Cells

To determine the source responsible for elevated serum CXCL1, we measured *Cxcl1* mRNA in different organs on α-Galcer injection. As shown in Figure 6*A*, great *Cxcl1* mRNA elevation was only observed in the liver but not in the heart, spleen, kidney, and lung after α-Galcer treatment. In line with above findings, the *Cxcl1* mRNA was higher in liver tissue of *Ccl5*^{-/-} mice than of WT mice, suggesting that the liver is the major source of *Cxcl1* induction in the α-Galcer–treated mice. It is worth noting that although *Cxcl2* mRNA levels were also induced in the liver of both strains after α-Galcer treatment, its expression did not show any difference between WT and *Ccl5*^{-/-} mice, suggesting that *Cxcl2* may not contribute to the increased hepatic neutrophil infiltration in *Ccl5*^{-/-} mice after α-Galcer treatment (Figure 6*B*).

Previous reports have indicated that both hepatocytes and NPCs in the liver can express CXCL1 in many pathogenic conditions.[31–33] To further investigate which cell types are responsible for CXCL1 production, we isolated hepatocytes and NPCs 3 hours after α-Galcer injection and detected *Cxcl1* mRNA in these cells. *Cxcl1* mRNA levels were elevated in
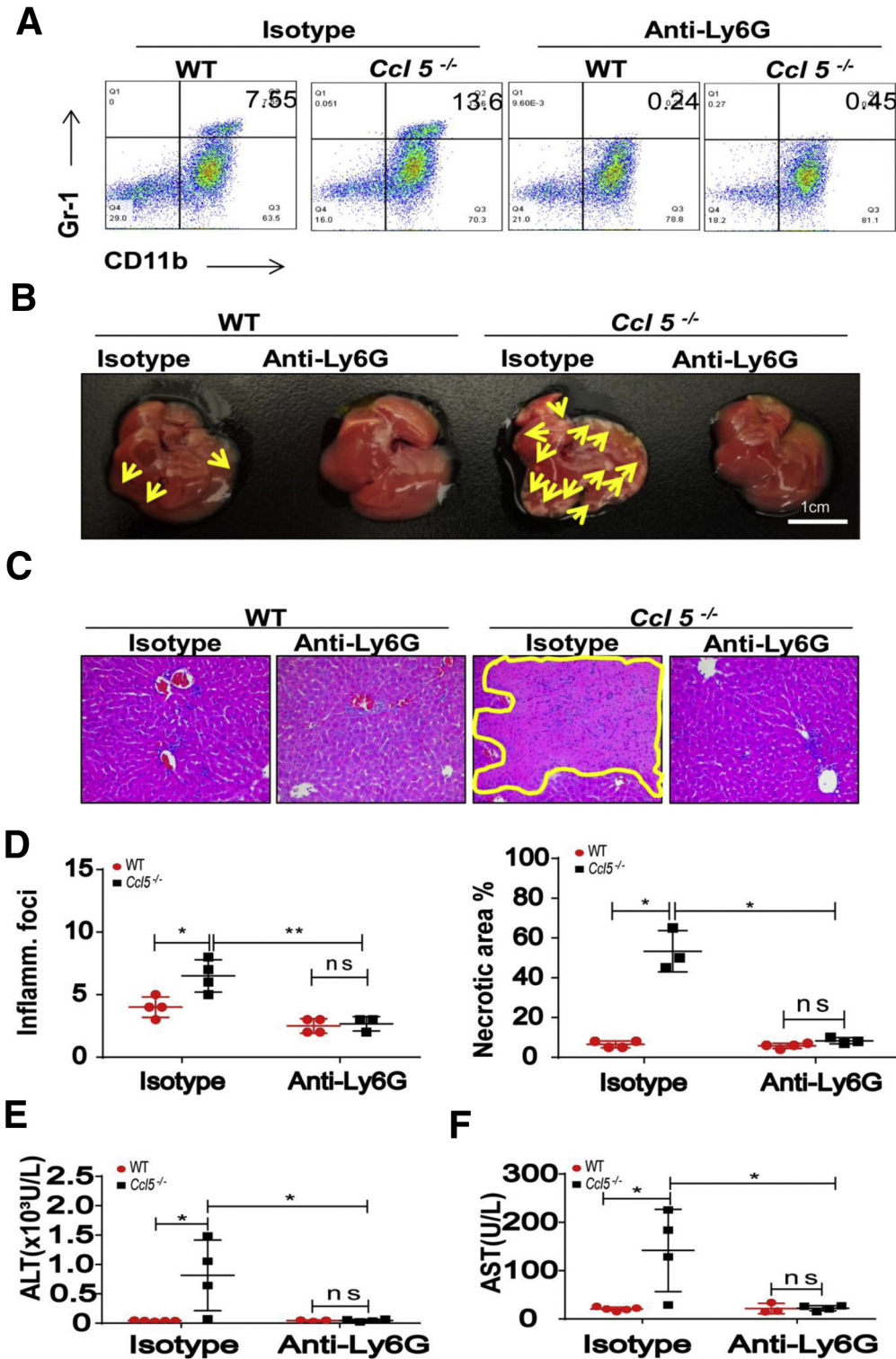
Figure 4. Enhanced a-Galcer–induced liver injury in *Ccl5*^{-/-} mice is dependent on nueutrophils. (*A*) WT and *Ccl5*^{-/-} mice were treated with isotype or anti-Ly6G antibodies 24 hours, followed by injection with α-Galcer. Mice were killed 24 hours after α-Galcer injection. Representative flow cytometry profiles showing percentages of neutrophils (CD11b^{high}Gr1^{high}) gated in CD45^{+} hepatic MNCs from each group. (*B*) Representative images of livers from each group of mice. (*C*) Representative H&E staining of liver tissue. (*D*) Graphs represent mean score of inflammatory foci and necrotic area for each group of mice. (*E*) Serum ALT levels were measured. (*F*) Serum AST levels were measured. *$P < .05$, **$P < .01$.

both hepatocytes and NPCs after α-Galcer treatment compared with untreated controls (Figure 6*C*). Interestingly, only the hepatocytes but not the NPCs from *Ccl5*^{-/-} mice showed greater *Cxcl1* induction after α-Galcer treatment (Figure 6*C*). Moreover, immunohistochemical staining of

CXCL1 in liver tissues also indicated that hepatocytes are the main source of α-Galcer–induced CXCL1 increase (Figure 6*E*). Similar to what we have observed in liver tissues, although *Cxcl2* mRNA was also elevated in both hepatocytes and NPCs from α-Galcer–treated mice, its
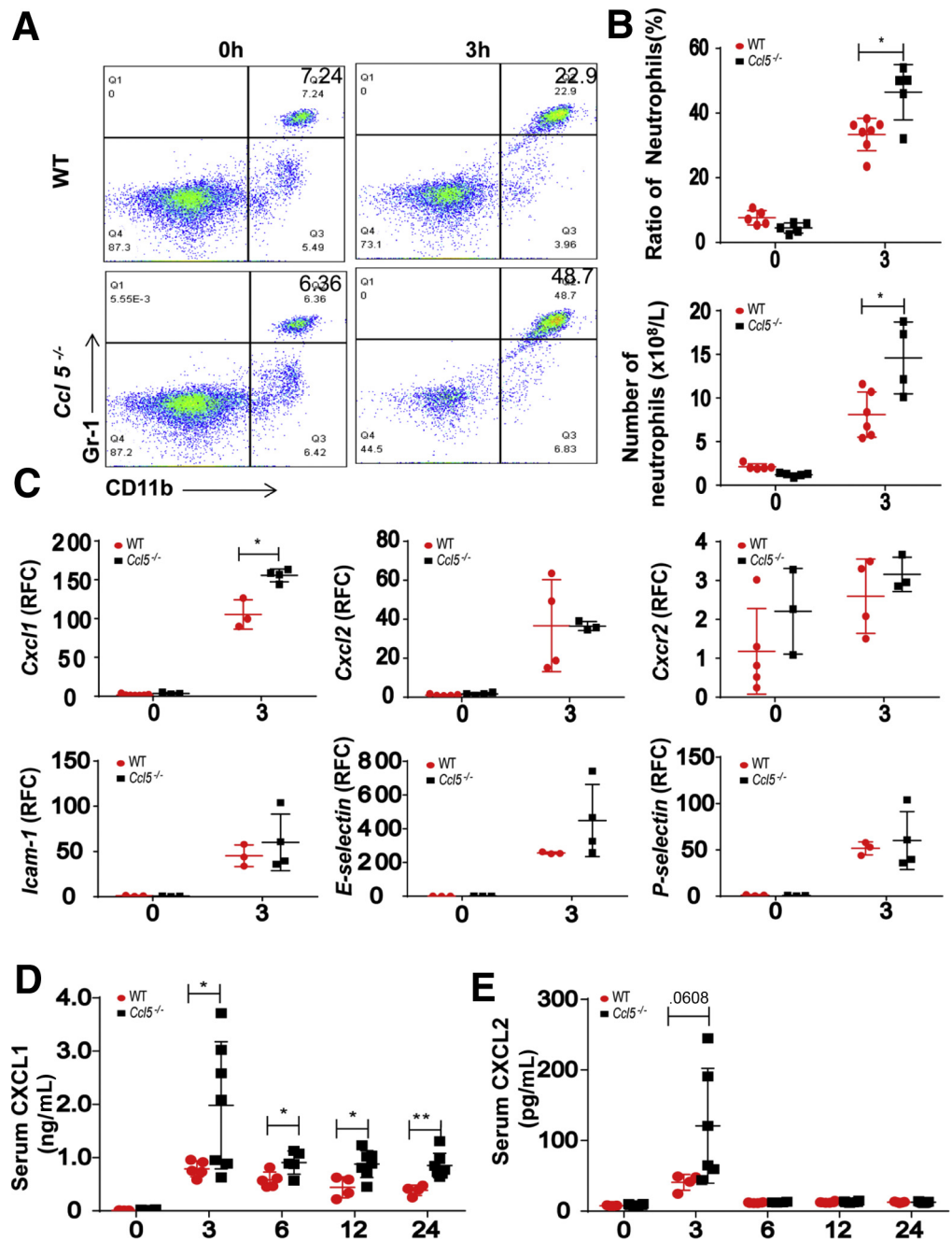
Figure 5. *Ccl5* deficiency synergistically up-regulates neutrophil infiltration in peripheral blood. (*A*) Representative flow cytometry profiles showing percentages of neutrophils (CD11b^high^Gr1^high^) gated in CD45^+^ peripheral blood cells from each group. (*B*) Proportion of neutrophils was shown, and total number of neutrophils was calculated. (*C*) Mice were treated with α-Galcer for 3 hours, liver tissues were collected, and total RNA was isolated and subjected to real-time PCR analysis of *Cxcl1*, *Cxcl2*, *Cxcr2*, *Icam-1*, *E-selectin*, and *P-selectin*. (*D*) Sera were collected to measure CXCL1 levels with ELISA kit. (*E*) Sera were collected to measure CXCL2 levels with ELISA kit. *$P < .05$.

induction showed no difference in both strains, further suggesting that *Cxcl2* does not contribute to the enhanced hepatic recruitment of neutrophils in *Ccl5^-/-^* mice (Figure 6*D*). Collectively, these findings indicate that hepatocytes produce higher CXCL1 in *Ccl5^-/-^* mice than in WT mice.

CCL5 transduces signals through its receptors CCR1, CCR3, and CCR5 in different biological processes. In the α-Galcer–induced hepatitis mouse model, *Ccr1* mRNA levels were much lower in both liver tissue and hepatocytes of *Ccl5^-/-^* mice than in WT mice 3 hours after α-Galcer treatment. However, no differences of CCR3 and CCR5 mRNA levels were found between *Ccl5^-/-^* and WT mice (Figure 6*F*

and *G*). These findings suggest that the lack of CCL5-CCR1 axis might cause increased CXCL1 production in *Ccl5^-/-^* mice in α-Galcer–induced hepatitis model.

The underlying mechanism of how *Ccl5* depletion results in elevation of hepatic CXCL1 remains unclear. We found the mRNA levels of peroxisome proliferator-activated receptor-γ, an inhibitor of the nuclear factor kappa B–CXCL1 axis, decreased 3 hours after α-Galcer stimulation in *Ccl5^-/-^* mice compared with WT mice (Figure 6*H*), suggesting that the reduced peroxisome proliferator-activated receptor-γ expression may confer a derepression on the nuclear factor kappa B–CXCL1 axis to induce Cxcl1 expression in *Ccl5^-/-^* mice.
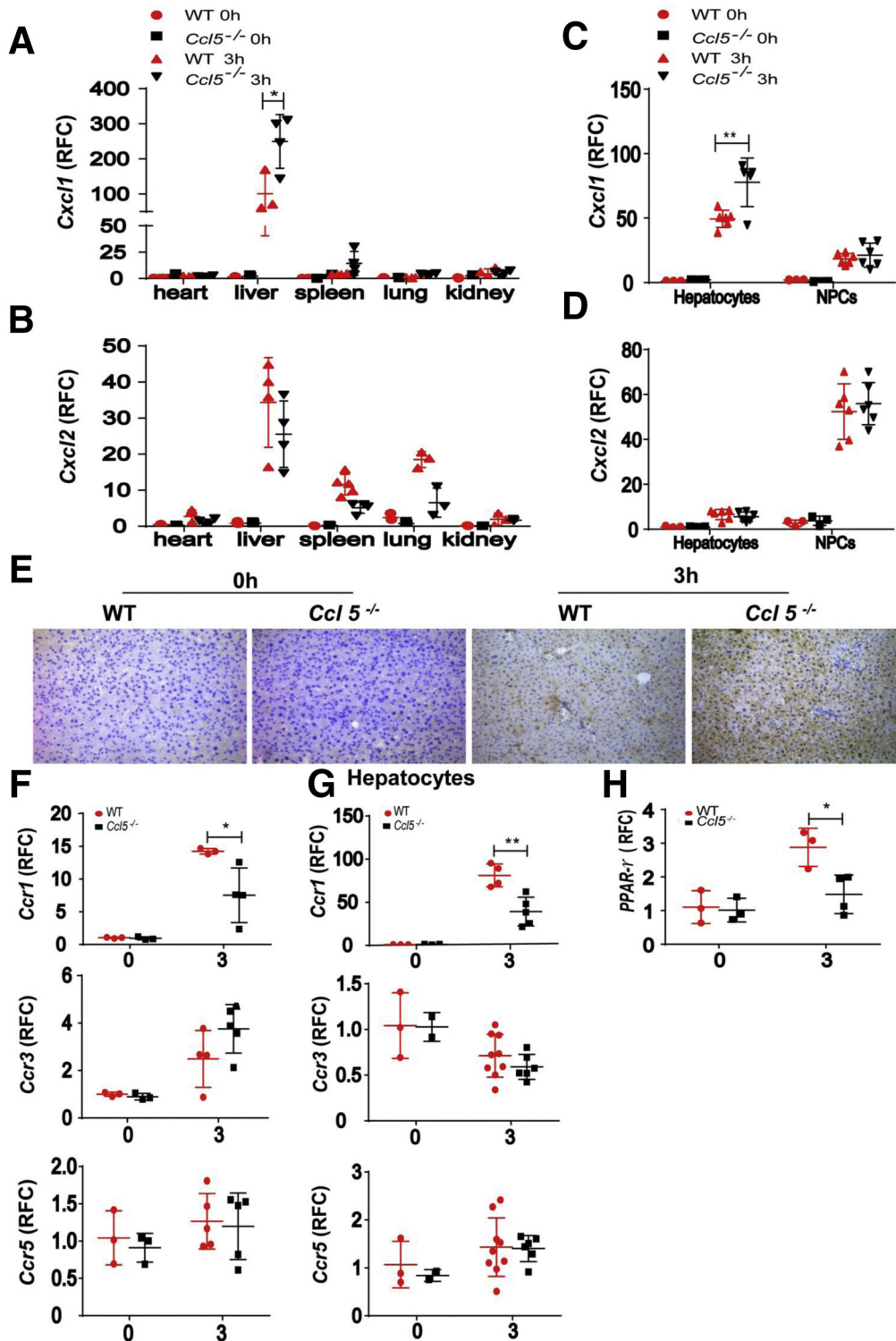
Figure 6. Up-regulation of *Cxcl1* mRNA expression in liver and hepatocytes from α-Galcer–treated *Ccl5*$^{-/-}$ mice. Mice were treated with α-Galcer for 3 hours, and various organs were collected and subjected to quantitative real-time PCR analysis of (*A*) *Cxcl1* and (*B*) *Cxcl2* mRNA. Hepatocytes and NPCs were isolated and subjected to real-time PCR analysis to determine levels of (*C*) *Cxcl1* and (*D*) *Cxcl2* mRNA. (*E*) Representative CXCL1 staining of liver tissue sections. (*F*) Quantitative real-time PCR analysis of *Ccr1*, *Ccr3,* and *Ccr5* in liver tissue from 3-hour α-Galcer treatment. (*G*) Quantitative real-time PCR analysis of *Ccr1*, *Ccr3,* and *Ccr5* in hepatocytes isolated from α-Galcer–treated mice for 3 hours. (*H*) Quantitative real-time PCR analysis of peroxisome proliferative-activated receptor-γ in liver tissue from 3-hour α-Galcer treatment. *$P <$ .05, **$P <$ .01.

Blocking the CXCL1-CXCR2 Axis Abolishes the Enhanced Liver Injury in C-C Motif Chemokine Ligand 5$^{-/-}$ Mice

To examine whether the increased CXCL1 levels contribute to the greater hepatic neutrophil infiltration and liver injury in *Ccl5*$^{-/-}$ mice after α-Galcer administration, we performed an in vitro migration assay to measure the chemotactic abilities of the serum from WT controls and *Ccl5*$^{-/-}$ mice 3 hours after α-Galcer treatment. As shown in Figure 7*A*, neutrophils were successfully purified by

magnetic separation. The serum from untreated WT and *Ccl5*^{-/-} mice showed weak and comparable chemotactic abilities on neutrophils (Figure 7*B* and *C*). As expected, the serum from α-Galcer–treated WT and *Ccl5*^{-/-} mice exhibited enhanced chemotactic abilities on neutrophils compared with untreated controls (Figure 7*B* and *C*). In line with our in vivo findings, the serum from α-Galcer–treated *Ccl5*^{-/-} mice displayed significantly greater chemotactic abilities on neutrophils than from WT mice (Figure 7*B* and *C*).

To examine whether CXCL1 is critical for the enhanced chemotactic ability on neutrophils in *Ccl5*^{-/-} mice, we blocked CXCL1 with an anti-CXCL1 antibody and observed a significant decrease in neutrophil chemotaxis in the serum from α-Galcer–treated *Ccl5*^{-/-} mice (Figure 7*D* and *F*). Because CXCL1 commonly interacts with a receptor CXCR2 to fulfill its chemotactic role on neutrophils, we then used a CXCR2 antagonist to block the CXCL1-CXCR2 axis. Similar to the findings in CXCL1 blockage by an anti-CXCL1 antibody, the enhanced neutrophil migration that was mediated by the serum from α-Galcer–treated *Ccl5*^{-/-} mice was greatly abolished by SB225002 (Figure 7*E* and *G*).

To further define the role of the CXCL1-CXCR2 axis in mediating enhanced liver injury in *Ccl5*^{-/-} mice after α-Galcer treatment, we first used anti-CXCL1 to neutralize the expression of CXCL1 in vivo. As shown in Figure 8*A* and *B*, anti-CXCL1 antibody could decrease higher ALT and AST in *Ccl5*^{-/-} mice. In addition, SB225002 treatment could alleviate macroscopic white spots, inflammatory foci, necrotic areas, and ALT/AST levels in *Ccl5*^{-/-} mice after α-Galcer treatment (Figure 8*C*–*G*). Therefore, our in vitro and in vivo assays suggest that the CXCL1-CXCR2 axis is responsible for the enhanced neutrophil recruitment and liver injury in *Ccl5*^{-/-} mice in the α-Galcer–induced mouse hepatitis model.

Discussion

The chemokine system directing the migration of immune cells via chemokine-chemokine receptor interaction has been reported in various types of liver diseases, including viral hepatitis, alcoholic hepatitis, fibrosis, HCC, as well as immune-mediated hepatitis.[3] In the present study, we demonstrate that CCL5 levels were significantly elevated in an α-Galcer–induced and iNKT activation mediated mouse hepatitis model, and genetic deletion of *Ccl5* exacerbated liver injury in this model. Intriguingly, higher accumulation of neutrophils was found in *Ccl5*^{-/-} mice, which was responsible for the enhanced liver injury and hepatitis. Furthermore, we found the hepatic infiltration of neutrophil was dependent on the CXCL1-CXCR2 axis, and hepatocytes were the main source of CXCL1 production.

In response to treatment, iNKTs produce a variety of IL4 and TNF-α (with a peak at 3 hours), followed by IFN-γ (with a peak at 16 hours), which orchestrate the infiltration and activation of other immune cells.[20,34] Mice treated with α-Galcer undergo mild hepatitis accompanied with elevated levels of liver transaminases and proinflammatory cytokines. In present study, we demonstrate that *Ccl5* ablation enhanced the aforementioned pathogenic effects of α-Galcer treatment in vivo. We first asked whether CCL5 could

directly regulate the activation status of iNKTs. Unexpectedly, the activation of iNKTs assessed by CD69 expression was comparable in both WT and *Ccl5*^{-/-} mice, suggesting that CCL5 has no direct effect on iNKT activation. Furthermore, the levels of iNKT cytokines IL4, TNF-α, and IFN-γ in *Ccl5*^{-/-} mice were also similar to those in WT mice after α-Galcer treatment. All these results indicate that there was no iNKT activation difference between WT and *Ccl5*^{-/-} mice after α-Galcer treatment.

Hepatic neutrophil infiltration has been demonstrated in promoting liver damage in a variety of liver diseases, including drug-induced liver injury (DILI), alcoholic liver injury, and high-fat diet plus ethanol-induced liver damage.[31] A previous study has also reported that the accumulation of neutrophils contributes to liver injury, and depletion of neutrophils protects from α-Galcer–induced liver injury.[20] The most striking finding in current study was that although activation status of iNKTs was not regulated by CCL5, hepatic neutrophil infiltration was elevated markedly in *Ccl5*^{-/-} mice as early as 3 hours after α-Galcer treatment. Moreover, after α-Galcer treatment, MNCs from *Ccl5*^{-/-} mice showed enhanced cytotoxicity on hepatocytes than those from WT mice, which provides direct evidence to explain why higher liver injury was observed in *Ccl5*^{-/-} mice than WT mice. Although blocking iNKT with anti-CD1d monoclonal antibody decreased the cytotoxicity of MNCs in both strains, the MNC-mediated cytotoxicity difference in both strains remains significant, further suggesting that the enhanced liver injury in α-Galcer–treated *Ccl5*^{-/-} mice is independent on iNKTs.

Because enhanced hepatic neutrophil infiltration is responsible for the higher liver injury in *Ccl5*^{-/-} mice, we examined the levels of chemokines that are well-defined to contribute to neutrophil infiltration. *Cxcl1*, a key chemokine in promoting neutrophil infiltration, was up-regulated in mRNA level by more than 100-fold and 150-fold in WT and CCL5^{-/-} mice liver tissue, respectively, after α-Galcer treatment. Furthermore, the serum CXCL1 levels were also elevated in *Ccl5*^{-/-} mice than WT mice. However, blockage of CXCL1 by a neutralizing antibody partially prevented hepatocellular damage. Considering other chemokines also contribute to neutrophils recruitment in vivo, we then used SB225002 to selectively block CXCR2, a receptor for both CXCL1 and CXCL2.[22] Blockage of CXCR2 could greatly ameliorate α-Galcer–induced liver injury in *Ccl5*^{-/-} mice. These results support that CCL5 deficiency leads to increased hepatic infiltration of neutrophils on α-Galcer treatment, which subsequently results in more severe liver injury.

De Filippo et al[35] reported that in lipopolysaccharide induced tissue inflammation, CXCL1/CXCL2 released by mast cells and macrophages regulated neutrophil recruitment at the early stage of inflammation. In our study, we further demonstrated that *Cxcl1* expression was up-regulated in hepatocytes and NPCs 3 hours after α-Galcer treatment, with the highest induction observed in hepatocytes. Considering that hepatocytes constitute the majority of the liver volume, we concluded that hepatocytes are largely responsible for the up-regulation of CXCL1 in the
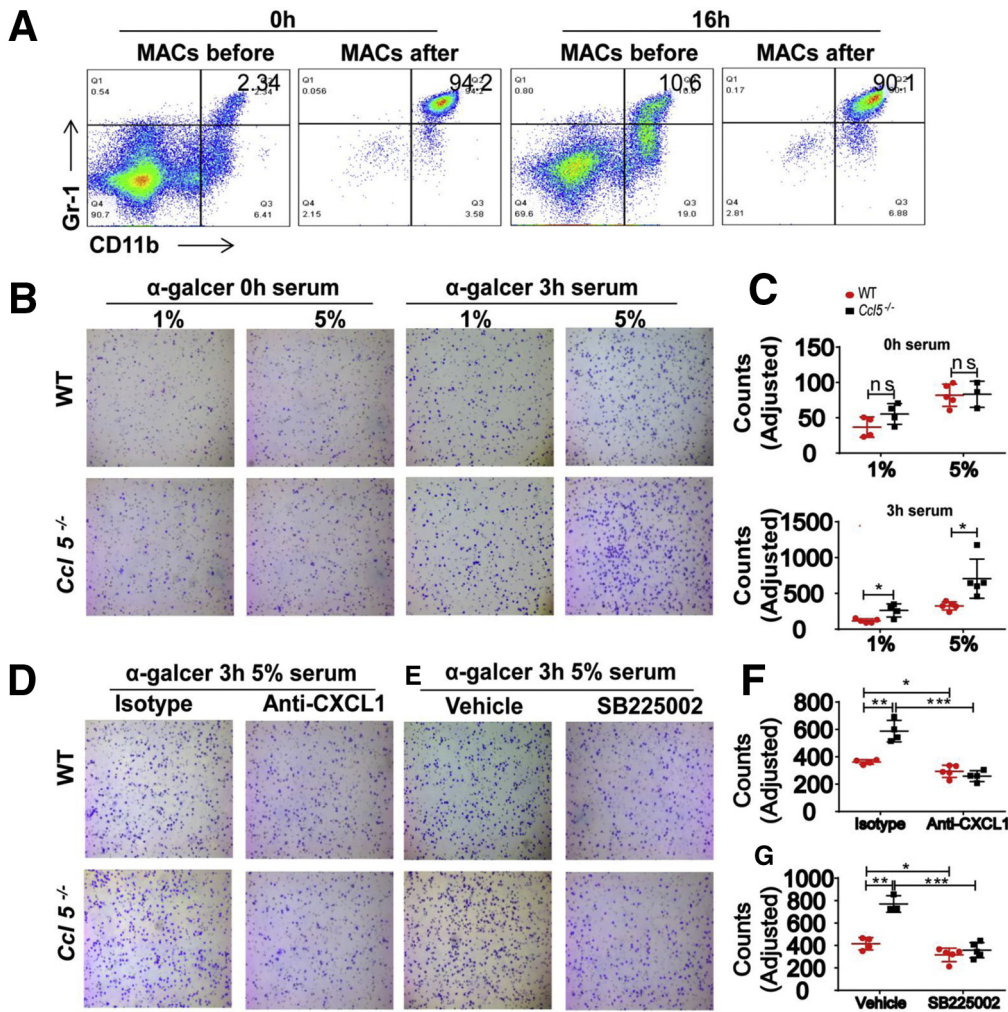
Figure 7. Augmented neutrophil recruitment is dependent on CXCL1 and CXCR2 mediated migration in an in vitro system. (*A*) Purity of MACS based isolation of neutrophil was verified by flow cytometry analysis. (*B*) Neutrophils isolated from α-Galcer–treated liver tissue were analyzed for their migration in response to 0-hour serum, 3-hour serum, or with anti-CXCL1 (*D*) or SB225002 (*F*). (*C, E,* and *G*) In magnification of ×100, 8–10 images of each group were taken randomly, and adjusted count was analyzed by Image-Pro Plus. *$P < .05$, **$P < .01$, ***$P < .001$.

liver after α-Galcer treatment. NPCs also contribute to this CXCL1 production but to a lesser extent. Indeed, the levels of other chemokines and adhesion molecules were comparable between the 2 strains. Moreover, the regulation role of CCL5 in neutrophil recruitment has been reported in a septic lung injury via promoting formation of CXCL2 in alveolar macrophages.[30] Despite that an opposite role of CCL5 in neutrophil recruitment was indicated here, we demonstrated a compensatory regulation between CCL5 and CXCL1.

In α-Galcer–induced hepatitis mouse model, Wang et al[20] found elevated neutrophil accumulation and enhanced liver injury after α-Galcer injection in *Ifn-γ*^{-/-} mice than WT mice. IL4 secreted by iNKT cells on α-Galcer treatment is responsible for neutrophil accumulation, and *Il4*^{-/-} mice are resistant to α-Galcer–induced liver injury and hepatitis compared with WT mice. In current study, we found no difference in IL4 between WT and *Ccl5*^{-/-} mice after α-Galcer treatment, suggesting that IL4 is not involved in the enhanced liver injury in *Ccl5*^{-/-} mice.

In the present study, we found that serum CCL5 levels were discrepant between patients with human

liver diseases (including HBV, HCV, and AIH) and the α-Galcer–induced hepatitis murine model. Human serum CCL5 levels were lower in those patients compared with healthy controls, whereas serum CCL5 levels were higher in mice treated with α-Galcer compared with vehicle controls. Two explanations may possibly address such discrepancy. (1) Alpha-Galcer–induced hepatitis murine model may not be equivalent to the pathology of chronic type B hepatitis (HBV), type C hepatitis (HCV), or AIH. (2) Serum CCL5 elevation may only happen in acute stage of liver injury. The patients recruited in current study have experienced long-term disease progression. Therefore, their liver injury should already be past the acute stage. Thus, the serum CCL5 levels should decrease from their peaks. In fact, we are currently investigating the role of CCL5 in acetaminophen-induced liver injury. In this project, we examined the serum CCL5 levels between healthy controls and patients with DILI. We found that the CCL5 levels in patients with DILI were significantly higher than those in healthy controls and positively associated with ALT levels, an indicator of acute liver injury (unpublished data). In addition, acute liver injury was observed in DILI patients but not in the patients

Figure 8. Blockade of CXCL1-CXCR2 axis diminished the enhanced hepatitis in *Ccl5*^{-/-} mice. (*A*) ALT and (*B*) AST were measured in serum from anti-CXCL1 and isotype control pretreatment mice, subsequently administered α-Galcer for 24 hours. WT and *Ccl5*^{-/-} mice were treated with vehicle or SB225002 for 1 hour, followed by injection with α-Galcer. (*C*) Macroscopic view of liver after SB225002 treatment. (*D*) Representative H&E staining of liver tissue was shown. (*E*) Graphs represent mean score of inflammatory foci and necrotic area for each group of mice. (*F*) Serum ALT levels were measured. (*G*) Serum AST levels were measured. $*P < .05$, $**P < .01$.
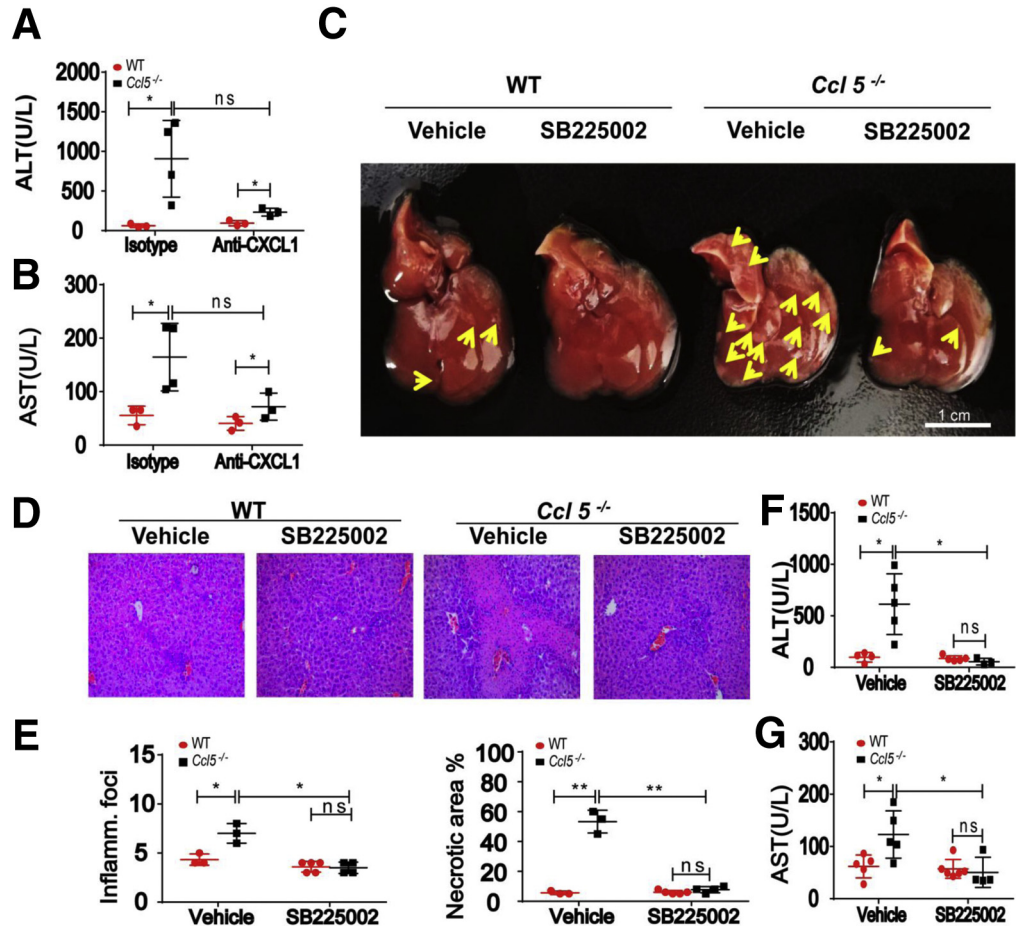
recruited in this study as evidenced by higher serum ALT levels in DILI patients compared with those HBV, HCV and AIH patients (unpublished data).

In summary, we found that deficiency of *Ccl5* may up-regulate CXCL1 production in hepatocytes and mediate higher hepatic infiltration of neutrophils, leading to greater liver injury in α-Galcer–induced murine hepatitis model. Thus, we conclude that the clinical use of blocking CCL5 may induce other chemokine signals such as CXCL1-CXCR2 to induce further enhanced hepatic infiltration of neutrophils. We further suggest that blocking CXCR2 or CXCL1 might be an effective way to control pathologic inflammation and tissue damage in hepatitis development.

Materials and Methods
Patients

Liver tissues with different etiologies, such as viral hepatitis B (HBV, n = 10), viral hepatitis C (HCV, n = 5), and AIH (n = 8) were collected from patients who received curative surgery, which were obtained from the Department of Liver Surgery, Renji Hospital, School of Medicine, Shanghai Jiaotong University. Normal control liver tissues (n = 10) were obtained from healthy donors during transplantation surgery. Informed consents from each patient were collected. Patient information is provided in Table 1.

Mice

WT and CCL5^{-/-} mice[36] (provided by Dr Yan Zhang, Renji-Med-X Stem Cell Research Center, Renji Hospital, China) on a C57/BL6 background were bred and maintained under specific pathogen-free conditions at the animal facility of Renji Hospital affiliated to Shanghai Jiao Tong University. Sex-matched mice were co-caged at weaning and used at age of 6–8 weeks. Animal studies were approved by the Institutional Animal Care and Use Committee of Shanghai Jiao Tong University, following the institutional guide for the care and use of laboratory animals.

Alpha-galactosylceramide–Induced Hepatitis Model in Mice

α-GalCer (cat number: BML-SL232, KRN7000; Enzo Life Science, Farmingdale, NY) was dissolved in 5.6% sucrose with 0.75% L-histidine and 0.5% Tween-20 and delivered intravenously via tail at 2 μg/mouse.

Table 1. Clinical Features of Patients

Etiology	Age (y)	Albumin (g/L)	ALT (U/L)	AST (U/L)	Alkaline phosphatase (U/L)	γ-glutamyl transpeptidase (U/L)	Direct bilirubin (μmol/L)	Total bilirubin (μmol/L)
HBV	49 (29, 65)	34.3 (26, 44.1)	152.8 (42.4, 1656)	162.5 (37.4, 3015)	85.5 (39, 178)	59 (15, 171)	50.75 (10.2, 361.6)	73.4 (35.4, 580.8)
HCV	54 (46, 59)	36.2 (26, 41.7)	96.8 (30, 345.1)	140 (22, 542.3)	97 (35, 142)	55.2 (23, 244.1)	25.1 (5, 35.1)	57.6 (14, 75)
AIH	52 (27, 66)	32.05 (22.6, 43.2)	69.25 (37, 377.1)	139.85 (52.6, 579)	145.5 (79, 219)	95.4 (50.6, 124)	87.75 (25.3, 247.8)	129.4 (39, 318.2)
Normal	24.5 (22, 33)	48.1 (40.8, 53.8)	17.5 (8, 53)	17 (11, 34)	79 (1.5, 166)	14.45 (10.2, 46.5)	3.6 (1.9, 6)	9.65 (6.1, 21.1)

NOTE. Data are presented as median (minimum, maximum).

Histologic Analysis

Four percent paraformaldehyde-fixed liver tissues were embedded in paraffin and cut in 5-μm thickness. The sections were subjected to H&E and immunohistochemistry staining. Antibodies used in immunohistochemistry staining included MPO (cat number: 901-023-100510; Biocare Medical, Concord, CA) and CXCL1 (cat number: BS-10234R; Bioss, Beijing, China).

Quantitative Real-time Polymerase Chain Reaction

Total RNA was extracted from liver tissue and liver cells by using the RNAiso Plus reagent (cat number: RP4002; Bioteke, Beijing, China). Five hundred ng total RNA was reverse-transcribed with the Hiscript II Reverse Transcriptase Kit (cat number: R223-01; Vazyme Biotech, Nanjing, China). The relative expression levels of genes to rplpo were measured by ChamQ SYBR qPCR Master Mix (cat number: Q311-02; Vazyme Biotech) and detected by CFX96 thermal Cycler (Bio-Rad, Hercules, CA).

Enzyme-linked Immunosorbent Assay

The levels of serum CCL5 (cat number: BMS6009INST; eBioscience, Inc, San Diego, CA), IFN-γ (cat number: EMC101g; Neobioscience, Shenzhen, China), IL4, CXCL1, and CXCL2 (cat number: EK2042/2, EK2962/2, EK1264, respectively; Lianke, Hangzhou, China) in supernatants were measured by using ELISA kit according to the manufacturer's instructions. Murine rCCL5, rIFN-γ, rIL4, rCXCL1 and rCXCL2 were used as standards.

Flow Cytometric Analysis

Mice were killed, and the livers were minced and tamped through the 70-μm nylon mesh. Liver leukocytes were purified by centrifugation on a 35% Percoll gradient, and remaining red blood cells were lysed by red blood cell lysis buffer (cat number:00-4333-57; eBioscience). For neutrophil detection, single-cell suspensions of MNCs were labeled with Fixable Viability Dyes eFluor 780 (cat number: 65-0865; eBioscience) and fluorescent conjugated antibodies against mouse CD 45.2 Alexa fluor 700 (cat number: 56-0454-82; eBioscience; clone: 104), Gr-1 FITC (cat number: 11-5931-85; eBioscience; clone: RB6-8C5), CD11b percp/cy 5.5 (cat number: 101228; BioLegend, San Diego, CA; clone: M1/70). For iNKT detection, single-cell suspensions of MNCs were labeled with fluorescent conjugated antibodies against mouse CD3-percp-efluor 710 (cat number: 46-0032-83; eBioscience; clone: 17A2) and NK1.1-APC (cat number: 17-5941-82; eBioscience; clone: PK136) or CD1d-tetramers-APC (National Institutes of Health core facility). Finally, flow cytometric analysis was performed according to standard settings on a CytoFLEX flow cytometer (Beckman Coulter, Fullerton, CA) and analyzed with Flowjo software (Treestar, Ashland, OR). A viable gate was used to exclude dead and fragmented cells.

Cytotoxicity Assay

Cytolytic activity of hepatic MNCs against primary hepatocytes was detected as previously described.[20] The

cytolytic activity was determined by EuTDA Cytotoxicity Reagents kit (cat number: AD0116; PerkinElmer, Waltham, MA) according to the manufacturer's protocols. Briefly, WT primary mouse hepatocytes were isolated and loaded with fluorescence enhancing ligand for 30 minutes at 37°C. The loaded hepatocytes were seeded on 96-well microtiter plates at a density of 1×10^4 cells/well. WT or CCL5$^{-/-}$ hepatic MNCs from 16-hour α-Galcer–treated mice were added onto primary hepatocytes at the ratio of 10:1 or 50:1. Meanwhile, 10 μg/mL anti-CD1d monoclonal antibody (cat number: BE0179; Bio X Cell, West Lebanon, NH) and rat immunoglobulin G1 isotype control (cat number: BE0290; Bio X Cell) were added in the medium. After 2 hours of incubation, the supernatant was collected and incubated with 200 μL Europium Solution. After incubation for 15 minutes at room temperature, the fluorescence was measured in a time-resolved fluorometer.

Anti-Ly6G Treatment

For neutrophil depletion, WT or CCL5$^{-/-}$ mice were intravenously administered 150 μg of either anti-mLy-6G (cat number: BE0075; 1A8; Bio X Cell) or isotype control antibody (cat number: BE0089; Rat IgG2a; Bio X Cell) 24 hours before α-Galcer treatment.

Neutrophil Chemotaxis

Neutrophils were isolated from liver tissue by using anti-Ly6G microbeads (cat number: 130-092-332; Miltenyi Biotec, Auburn, CA). Two times 10^5 neutrophils were placed in the upper chamber of the Transwell inserts with a pore size of 5 μm (Falcon inserts; Corning Incorporated, Corning, NY), which were loaded in wells containing medium plus 1% or 5% serum from control or α-Galcer–treated mice. In ablation experiments, anti-CXCL1 (cat number: MAB453; 500 ng/mL; R&D Systems, Minneapolis, MN) or CXCR2 antagonist SB225002 (cat number: HY-16711; 2 μmol/mL; MedChem Express, Monmouth Junction, NJ) and their corresponding control were added into the medium. Two hours later, inserts were removed and stained with crystal violet. Migrated neutrophils were counted by Image-Pro Plus; Media Cybernetics, Rockville, MD).

Hepatocytes, Macrophages, and Hepatic Stellate Cells Isolation

Primary macrophages and HSCs were obtained by in situ perfusion. Briefly, the liver was perfused via portal vein with 40 mL EGTA buffer (5.4 mmol/L KCl, 0.44 mmol/L KH2PO4, 0.338 mmol/L Na2HPO4, 137 mmol/L NaCl, 25 mmol/L Tricine, and 0.5mmol/L EGTA) for 5 minutes, followed by Gey's balanced saline solution (GBSS) (2 mmol/L CaCl2, 1 mmol/L MgCl2, 0.285 mmol/L MgSO4, 5 mmol/L KCl, 0.20 mmol/L KH2PO4, 27 mmol/L NaHCO3, 120 mmol/L NaCl, 0.8 mmol/L Na2HPO4, 5.6 mmol/L D-glucose) containing 40 mL 0.075% collagenase I (cat number: C0130; Sigma-Aldrich, St Louis, MO) for 5 minutes. Then the liver was dissociated with a digestion GBSS buffer containing collagenase IV (0.008%) for 5 minutes at 37°C and filtered through a 70-μm nylon cell strainer. After being centrifuged at 500 rpm for 5 minutes, the hepatocyte pellets were collected for the following use.

The supernatant (NPCs) was performed for density gradient centrifugation for isolation of Kupffer cells or HSCs, respectively. For HSCs isolation, the NPCs were centrifuged by density gradient 12.5% OptiPrep (cat number: D1556; Sigma-Aldrich). The HSCs were collected for the following RNA extract.

For macrophage isolation, the NPCs were laid on a 25%/50% two-step Percoll (cat number: 17-0891-09; Amersham, Stockholm, Sweden) gradient, 1800g for 17 minutes at room temperature, and collected the middle layer and plate in non-collagen–coated culture plate (6-well plate) for 15–20 minutes. The debris and unattached cells were removed. The attached cells were collected for RNA extract and immunofluorescent assay.

Immune Cell Isolation From Bone Marrow

Mice were killed and sterilized with 70% ethanol at abdomen area and skin of hindlimbs. The femur and tibia bones of mice were obtained carefully and cut at both ends with sharp sterile scissors. A 1-mL syringe filled with ice-cold RPMI 1640 was used to flush the bone marrow onto a 40-μm nylon cell strainer placed in a 50-mL tube, and the flush was repeated until the flow through turned white. Subsequently, the red blood cells were lysed by RBC lysis buffer (cat number: 00-4333-57; eBioscience). Immune cells were stained and detected by CytoFLEX flow cytometer (Beckman Coulter). In addition to the antibodies mentioned before, the antibodies used here included CD19-FITC (cat number: 12-0193-81; eBioscience; clone: BM-19-1), CD11c FITC (cat number: 11-0114-81; eBioscience; clone: N418), and F4/80 efluor 450 (cat number: 48-4801-82; eBioscience; clone: BM8).

Splenocyte Isolation

The whole spleen was extracted from mice and placed in a 6-cm dish. The spleen was tamped with the rubber end of a plunger from a 5-mL syringe against the 40-μm nylon cell strainer to make single cells. Subsequently, the red blood cells were lysed by RBC lysis buffer. Splenocytes were stained as mentioned above and detected by CytoFLEX flow cytometer.

Natural Killer T-Cell Isolation

The isolation of NKT cells was performed by magnetic purification with NK1.1+ iNKT Cell Isolation Kit (cat number: 130-096-513; Miltenyi Biotec). In brief, the liver MNCs were labeled with a cocktail of biotin-conjugated antibodies and anti-biotin microbeads. The labeled cells were subsequently depleted by separation over a LD column, which is placed in the magnetic field of a MACS Separator (Miltenyi Biotec). The unlabeled cells were collected and subjected to the second step. The cells were labeled with anti-NK1.1-APC and anti-APC microbeads. After incubation, the cells were isolated by positive selection from the pre-enriched cell fraction by separation over a LS column, which is placed in the magnetic field of a MACS Separator. After removing the

column from the magnetic field, the NK1.1+ iNKT cells can be eluted as the positively selected cell fraction.

Immunofluorescent Assay

The isolated NKT cells were fixed with 4% formaldehyde for 20 minutes at room temperature and smeared on a gelatin-coated slide. After the liquid evaporated, the slide was washed with water until there were no salt crystals. The cells were stained by mouse CCL5/RANTES antibody (cat number: AF478; R&D System) and visualized by Alexa Fluor 488 AffiniPure Donkey anti-goat immunoglobulin G (H+L) Alexa Fluor 488 (cat number: 34306ES60; Yeasen, Shanghai, China).

In Vivo Administration of SB225002

WT or CCL5$^{-/-}$ mice were administered intraperitoneally with vehicle or a CXCR2 antagonist SB225002 (cat number: HY-16711; 4 mg/kg; MedChem Express) 2 hours before α-Galcer treatment.

Relative Quantification of Neutrophil Extracellular Traps

NET formation in serum was determined by MPO-DNA complex, which was developed as previously. A capture antibody to MPO (cat number: HK210-01, coated strips; Hycult Biotech, Plymouth Meeting, PA) and detection antibody to DNA (cat number: 11774424001, component No. 2; Cell Death ELISA, Roche Biotech, Basel, Switzerland) were used according to manufacturer's instructions.

In vitro Neutrophil Extracellular Trap Formation

Bone marrow derived neutrophils were isolated by MACS (cat number: 130-092-332; Miltenyi Biotec) and plated to adhere in polylysine coated plates for 1 hour. After that, the neutrophils from both strains were stimulated for 4 hours with phorbol 1,2-myristate 1,3-acetate (100 nmol/L; cat number: P1585; Sigma-Aldrich). The cells were fixed and stained by cit-histone (cat number: ab5103; Abcam, Cambridge, MA) for 2 hours at room temperature. Alexa Fluor 594-goat anti-rabbit immunoglobulin G (cat number: 515-585-003; Jackson ImmunoResearch, West Grove, PA) was used as a secondary antibody. Slides were visualized by fluorescence microscopy (Leica, Buffalo Grove, IL).

Liver Damage Assessment

Serum levels of ALT (cat number: C009-2) and AST (cat number: C010-2) were quantified by biochemical detection kit from Jiancheng Bioengineering Institute (Nanjing, China).

Statistical Analysis

In this study, all data were presented as mean values ± standard deviation. Comparisons of 2 groups were performed by using the unpaired *t* test. *P* value <.05 was considered statistically significant. Statistical analysis was performed by GraphPad Prism 6 software (GraphPad Software, San Diego, CA).

References

1. Marra F, Tacke F. Roles for chemokines in liver disease. Gastroenterology 2014;147:577–594.
2. Charo IF, Ransohoff RM. The many roles of chemokines and chemokine receptors in inflammation. N Engl J Med 2006;354:610–621.
3. Marra F. Chemokines in liver inflammation and fibrosis. Front Biosci 2002;7:d1899–d1914.
4. Marques RE, Guabiraba R, Russo RC, Teixeira MM. Targeting CCL5 in inflammation. Expert Opin Ther Targets 2013;17:1439–1460.
5. Lee C, Peng H, Yang P, Liou J, Liao C, Day Y. C-C chemokine ligand-5 is critical for facilitating macrophage infiltration in the early phase of liver ischemia/reperfusion injury. Scientific Reports 2017;7:3698.
6. Park JH, Lee DH, Park MS, Jung YS, Hong JT. CCR5 deficiency exacerbates alcoholic fatty liver disease through pro-inflammatory cytokines and chemokines-induced hepatic inflammation. J Gastroenterol Hepatol 2016;32:1258–1264.
7. Ajuebor MN, Wondimu Z, Hogaboam CM, Le T, Proudfoot AEI, Swain MG. CCR5 deficiency drives enhanced natural killer cell trafficking to and activation within the liver in murine T cell-mediated hepatitis. Am J Pathol 2007;170:1975–1988.
8. Moreno C, Gustot T, Nicaise C, Quertinmont E, Nagy N, Parmentier M, Le Moine O, Devière J, Louis H. CCR5 deficiency exacerbates T-cell-mediated hepatitis in mice. Hepatology 2005;42:854–862.
9. Berres ML, Koenen RR, Rueland A, Zaldivar MM, Heinrichs D, Sahin H, Schmitz P, Streetz KL, Berg T, Gassler N, Weiskirchen R, Proudfoot A, Weber C, Trautwein C, Wasmuth HE. Antagonism of the chemokine Ccl5 ameliorates experimental liver fibrosis in mice. J Clin Invest 2010;120:4129–4140.
10. Stock MK, Hammerich L, Do ON, Berres ML, Alsamman M, Heinrichs D, Nellen A, Trautwein C, Tacke F, Wasmuth HE, Sahin H. Met-CCL5 modifies monocyte subpopulations during liver fibrosis regression. Int J Clin Exp Pathol 2013;6:678–685.
11. Perez-Martinez L, Perez-Matute P, Aguilera-Lizarraga J, Rubio-Mediavilla S, Narro J, Recio E, Ochoa-Callejero L, Oteo JA, Blanco JR. Maraviroc, a CCR5 antagonist, ameliorates the development of hepatic steatosis in a mouse model of non-alcoholic fatty liver disease (NAFLD). J Antimicrob Chemother 2014; 69:1903–1910.
12. Mohs A, Kuttkat N, Reissing J, Zimmermann HW, Sonntag R, Proudfoot A, Youssef SA, de Bruin A, Cubero FJ, Trautwein C. Functional role of CCL5/RANTES for HCC progression during chronic liver disease. J Hepatol 2017;66:743–753.
13. Koh MY, Gagea M, Sargis T, Lemos RJ, Grandjean G, Charbono A, Bekiaris V, Sedy J, Kiriakova G, Liu X, Roberts LR, Ware C, Powis G. A new HIF-1alpha/RANTES-driven pathway to hepatocellular carcinoma mediated by germline haploinsufficiency of SART1/HAF in mice. Hepatology 2016;63:1576–1591.

14. Wang H, Yin S. Natural killer T cells in liver injury, inflammation and cancer. Expert Review of Gastroenterology & Hepatology 2015;9:1077–1085.

15. Godfrey DI, Hammond KJL, Poulton LD, Smyth MJ, Baxter AG. NKT cells: facts, functions and fallacies. Immunol Today 2000;21:573–583.

16. Zhu S, Zhang H, Bai L. NKT cells in liver diseases. Frontiers of Medicine 2018;12:249–261.

17. Santodomingo-Garzon T, Swain MG. Role of NKT cells in autoimmune liver disease. Autoimmun Rev 2011; 10:793–800.

18. Kronenberg M, Gapin L. The unconventional lifestyle of NKT cells. Nat Rev Immunol 2002;2:557–568.

19. Schneiders FL, Scheper RJ, von Blomberg BME, Woltman AM, Janssen HLA, van den Eertwegh AJM, Verheul HMW, de Gruijl TD, van der Vliet HJ. Clinical experience with α-galactosylceramide (KRN7000) in patients with advanced cancer and chronic hepatitis B/C infection. Clin Immunol 2011;140:130–141.

20. Wang H, Feng D, Park O, Yin S, Gao B. Invariant NKT cell activation induces neutrophil accumulation and hepatitis: opposite regulation by IL-4 and IFN-r. Hepatology 2013; 58:1474–1485.

21. Dienes H, Drebber U. Pathology of immune-mediated liver injury. Dig Dis 2010;28:57–62.

22. Karlmark KR, Wasmuth HE, Trautwein C, Tacke F. Chemokine-directed immune cell infiltration in acute and chronic liver disease. Expert Review of Gastroenterology & Hepatology 2014;2:233–242.

23. Lisbonne M, Diem S, de Castro KA, Lefort J, Araujo LM, Hachem P, Fourneau JM, Sidobre S, Kronenberg M, Taniguchi M, Van Endert P, Dy M, Askenase P, Russo M, Vargaftig BB, Herbelin A, Leite-de-Moraes MC. Cutting edge: invariant V alpha 14 NKT cells are required for allergen-induced airway inflammation and hyperreactivity in an experimental asthma model. J Immunol 2003; 171:1637–1641.

24. Wilson MT, Johansson C, Olivares-Villagomez D, Singh AK, Stanic AK, Wang CR, Joyce S, Wick MJ, Van Kaer L. The response of natural killer T cells to glycolipid antigens is characterized by surface receptor down-modulation and expansion. Proc Natl Acad Sci U S A 2003;100:10913–10918.

25. Xu R, Huang H, Zhang Z, Wang FS. The role of neutrophils in the development of liver diseases. Cell Mol Immunol 2014;11:224–231.

26. Huang H, Tohme S, Al-Khafaji AB, Tai S, Loughran P, Chen L, Wang S, Kim J, Billiar T, Wang Y, Tsung A. Damage-associated molecular pattern-activated neutrophil extracellular trap exacerbates sterile inflammatory liver injury. Hepatology 2015;62:600–614.

27. Honda M, Kubes P. Neutrophils and neutrophil extracellular traps in the liver and gastrointestinal system. Nature Reviews Gastroenterology & Hepatology 2018; 15:206–221.

28. Honczarenko M. CCR5-binding chemokines modulate CXCL12 (SDF-1)-induced responses of progenitor B cells in human bone marrow through heterologous desensitization of the CXCR4 chemokine receptor. Blood 2002;100:2321–2329.

29. Rossi D, Zlotnik A. The biology of chemokines and their receptors. Annu Rev Immunol 2000;18:217–242.

30. Hwaiz R, Rahman M, Syk I, Zhang E, Thorlacius H. Rac1-dependent secretion of platelet-derived CCL5 regulates neutrophil recruitment via activation of alveolar macrophages in septic lung injury. J Leukoc Biol 2015; 97:975–984.

31. Chang B, Xu M, Zhou Z, Cai Y, Li M, Wang W, Feng D, Bertola A, Wang H, Kunos G, Gao B. Short- or long-term high-fat diet feeding plus acute ethanol binge synergistically induce acute liver injury in mice: an important role for CXCL1. Hepatology 2015; 62:1070–1085.

32. Li X, Klintman D, Liu Q, Sato T, Jeppsson B, Thorlacius H. Critical role of CXC chemokines in endotoxemic liver injury in mice. J Leukoc Biol 2004;75:443–452.

33. Wang W, Xu M, Cai Y, Zhou Z, Cao H, Mukhopadhyay P, Pacher P, Zheng S, Gonzalez FJ, Gao B. Inflammation is independent of steatosis in a murine model of steatohepatitis. Hepatology 2017;66:108–123.

34. Gao B, Radaeva S, Park O. Liver natural killer and natural killer T cells: immunobiology and emerging roles in liver diseases. J Leukoc Biol 2009;86:513–528.

35. De Filippo K, Dudeck A, Hasenberg M, Nye E, van Rooijen N, Hartmann K, Gunzer M, Roers A, Hogg N. Mast cell and macrophage chemokines CXCL1/CXCL2 control the early stage of neutrophil recruitment during tissue inflammation. Blood 2013;121:4930–4937.

36. Zhang Q, Qin J, Zhong L, Gong L, Zhang B, Zhang Y, Gao WQ. CCL5-mediated Th2 immune polarization promotes metastasis in luminal breast cancer. Cancer Res 2015;75:4312–4321.

Correspondence
Address correspondence to: Hailong Wu, PhD, Shanghai Key Laboratory for Molecular Imaging, Collaborative Research Center, Shanghai University of Medicine and Health Sciences, Shanghai, China. e-mail: wuhailong2@hotmail.com; fax: +86 21 587 372 32; or Xiaoni Kong, PhD, e-mail: xiaoni-kong@126.com.